Available online at www.sciencedirect.com
ScienceDirect
Computers and Mathematics with Applications 55 (2008) 1433–1440
An International Journal
computers & mathematics
with applications
www.elsevier.com/locate/camwa

The lattice Boltzmann method for the thermocapillary flow in a cavity under microgravity condition

Rui Du[a], Baochang Shi[b,*]

[a] State Key Laboratory of Coal Combustion, Huazhong University of Science and Technology, 1037 Luoyu Road, Wuhan, 430074, China
[b] Department of Mathematics, Huazhong University of Science and Technology, 1037 Luoyu Road, Wuhan, 430074, China

Abstract

In this paper an LBGK model for thermocapillary flow in microgravity is proposed. In the model two distribution functions are used for the velocity and temperature fields, respectively. Through the Chapman–Enskog expansion, the macroscopic equations for the thermocapillary flow can be recovered from the LBGK model. The boundary conditions for the thermocapillary flow are treated using the non-equilibrium extrapolation scheme. The model is validated by simulating the thermocapillary flow in a two-dimensional (2D) square cavity with a single free surface and differentially heated side walls.

Keywords: Lattice Boltzmann method; Thermocapillary flow; Microgravity

1. Introduction

Convective flows driven by the surface tension due to a temperature gradient are of considerable interest and play an important role in small-scale and/or low-gravity hydrodynamics. Because these thermocapillary flows usually occur on crystal growth melts and dominate the convective flows in the microgravity environment of space, there have been a number of studies using simplified 2D models with negligible gravitational effects [1–7]. Many traditional methods, such as the finite-difference methods and finite-volume methods, have been applied to solve such problems. In this paper, an alternative method, the lattice Boltzmann BGK (LBGK) model [8], is employed to simulate this problem. The LBGK model is a relatively new approach that uses simple microscopic kinetic models to simulate complicated macroscopic behaviors of transport phenomena [9–11]. From a computational viewpoint, the notable advantages of the LBGK are the intrinsic parallelism of algorithm, the simplicity of programming, and the ease of incorporating microscopic interactions.

The LBGK model for the thermocapillary flow with microgravity used in the present work is constructed based on the idea of the double distribution functions (DDF) LB model for natural convection equations [12,13]. In this model, the incompressible LBGK model [14] is used to model the incompressible Navier–Stokes equations, and an

* Corresponding author.
E-mail addresses: duruimail@gmail.com (R. Du), sbchust@yahoo.com (B. Shi).

0898-1221/$ - see front matter © 2007 Elsevier Ltd. All rights reserved.
doi:10.1016/j.camwa.2007.08.008

additional LBGK equation is used to describe the evolution of the temperature field [12,13]. The model is validated by simulating a 2D thermocapillary flow in a rectangular cavity with a single free surface and differentially heated side walls, where the ZHM model [2] is used so that the free surface can be assumed to remain flat at leading order. Numerical simulations have been carried on with different Reynolds numbers and the relative height of the external temperature on the left wall. The numerical results agree well with other existing results [7].

2. The LBGK model for thermocapillary flows

The dimensionless equations for a thermocapillary flow in the absence of gravity read

$$\nabla \cdot \mathbf{u} = 0, \tag{1a}$$

$$\frac{\partial \mathbf{u}}{\partial t} + \mathbf{u} \cdot \nabla \mathbf{u} = -\nabla p + \frac{1}{Re}\nabla^2 \mathbf{u}, \tag{1b}$$

$$\frac{\partial \Theta}{\partial t} + \mathbf{u} \cdot \nabla \Theta = \frac{1}{Ma}\nabla^2 \Theta, \tag{1c}$$

where $\mathbf{u}$, θ and p is the dimensionless velocity, temperature and pressure of the flow, respectively. The characteristic length and velocity are h and $U_0 = |\sigma_T|\Delta T_\parallel/\rho\nu$, where $\sigma_T = \frac{\partial \sigma}{\partial T}$ is the gradient coefficient of surface tension σ, ρ is the density of the flow, ν is the kinetic viscosity and $\Delta T_\parallel$ is the temperature difference along the horizontal direction. Re, Ma and Pr are the Reynolds number, Marangoni number and Prandtl number, respectively, and are defined as

$$Re = \frac{U_0 h}{\nu}, \qquad Ma = \frac{U_0 h}{\kappa}, \qquad Pr = \frac{\nu}{\kappa} = \frac{Ma}{Re}, \tag{2}$$

where κ is the thermal diffusivity.

For a 2D problem, we can solve the governing equations (1) using a 2D nine-bit (D2Q9) LBGK model, where the discrete velocities are defined as,

$$\mathbf{e}_i = \begin{cases} (0,0) & i = 0 \\ (\cos[(i-1)\pi/2], \sin[(i-1)\pi/2])c & i = 1,\ldots,4 \\ \sqrt{2}(\cos[(i-1)\pi/2+\pi/4], \sin[(i-1)\pi/2+\pi/4])c & i = 5,\ldots,8. \end{cases} \tag{3}$$

In order to solve the Eq. (1) in the LBGK framework, we follow the idea of the two distribution function similar to that used in [12,13]. Specifically, the velocity field is described by the incompressible D2Q9 model [14], and the temperature field is described by the D2Q4 model. The two LBGK equations read

$$g_i(\mathbf{x} + \mathbf{e}_i\Delta t, t + \Delta t) - g_i(\mathbf{x}, t) = -\tau_u^{-1}(g_i(\mathbf{x}, t) - g_i^{\mathrm{eq}}(\mathbf{x}, t)) \quad \text{for } i = 0,\ldots,8, \tag{4a}$$

$$\Theta_i(\mathbf{x} + \mathbf{e}_i\Delta t, t + \Delta t) - \Theta_i(\mathbf{x}, t) = -\tau_T^{-1}(\Theta_i(\mathbf{x}, t) - \Theta_i^{\mathrm{eq}}(\mathbf{x}, t)) \quad \text{for } i = 1,\ldots,4, \tag{4b}$$

where $c = \Delta x/\Delta t$ is the particle speed, Δx and Δt are the lattice grid spacing and time step, respectively. $g_i(\mathbf{x}, t)$ and $\Theta_i(\mathbf{x}, t)$ are the distribution functions at computing node $\mathbf{x}$ and time t. $g_i^{\mathrm{eq}}(\mathbf{x}, t)$ and $\Theta_i^{\mathrm{eq}}(\mathbf{x}, t)$ are the equilibrium functions accordingly. In this paper, $g_i^{\mathrm{eq}}(\mathbf{x}, t)$ proposed by Guo [14] are defined

$$g_i^{\mathrm{eq}} = \begin{cases} \rho_0 - (1-\omega_0)\dfrac{p}{c_s^2} + s_0(\mathbf{u}), & i = 0 \\ \omega_i \dfrac{p}{c_s^2} + s_i(\mathbf{u}), & i = 1,\ldots,8 \end{cases} \tag{5}$$

where

$$s_i(\mathbf{u}) = \omega_i\left[\frac{\mathbf{e}_i \cdot \mathbf{u}}{c_s^2} + \frac{(\mathbf{e}_i \cdot \mathbf{u})^2}{2c_s^2} - \frac{|\mathbf{u}|^2}{2c_s^2}\right], \tag{6}$$

with the weight coefficient $\omega_0 = 4/9, \omega_{1-4} = 1/9, \omega_{5-8} = 1/36$ and $c_s = c/\sqrt{3}$ is the speed of sound. ρ_0 is a constant.

$\Theta_i^{\mathrm{eq}}(\mathbf{x}, t)$ are defined as

$$\Theta_i^{\mathrm{eq}}(\mathbf{x}, t) = \frac{\Theta}{4}\left[1 + 2\frac{\mathbf{e}_i \cdot \mathbf{u}}{c^2}\right], \quad i = 1, \ldots, 4. \tag{7}$$

The macroscopic velocity, pressure and temperature of the flow are defined as

$$\mathbf{u} = \sum_{i=1}^{8} \mathbf{e}_i g_i = \sum_{i=1}^{8} \mathbf{e}_i g_i^{\mathrm{eq}}, \tag{8a}$$

$$p = \frac{c_s^2}{1-\omega_0}\left[\sum_{i=1}^{8} g_i + s_0(\mathbf{u})\right] = \frac{c_s^2}{1-\omega_0}\left[\sum_{i=1}^{8} g_i^{\mathrm{eq}} + s_0(\mathbf{u})\right], \tag{8b}$$

$$\Theta = \sum_{i=1}^{4} \Theta_i = \sum_{i=1}^{4} \Theta_i^{\mathrm{eq}}. \tag{8c}$$

It is noted that the constant ρ_0 takes no effect in the computations of the macroscopic quantities and is set to be 1.0 in the numerical simulations.

Through the Chapman–Enskog expansion [13,14], the macroscopic equations can be derived from the LBGK model with

$$\nu = \frac{1}{3}\left(\tau_u - \frac{1}{2}\right)\frac{\Delta x^2}{\Delta t}, \tag{9a}$$

$$\kappa = \frac{1}{2}\left(\tau_T - \frac{1}{2}\right)\frac{\Delta x^2}{\Delta t}. \tag{9b}$$

3. Numerical results

3.1. Problem description

The problem we considered is the thermocapillary flow in a square cavity filled with melt in the absence of gravitational force (See Fig. 1). The motion is referred to a Cartesian coordinate system with the origin at the left of the bottom boundary and with the y axis parallel to the side walls. The top horizontal boundary is a free surface.

In the range $h - h_1 \le y \le h$, the vertical walls of the cavity keep the temperature T_L and T_R for the left and right walls, respectively. T_B is the temperature of the bottom. Let $\Theta = (T - T_R)/\Delta T_\perp$, the dimensionless temperature is $\Delta T_\parallel/\Delta T_\perp$ and 0 for the left and right walls, respectively, where $\Delta T_\parallel = T_L - T_R$ and $\Delta T_\perp = T_R - T_B$.

The flow is governed by Eq. (1), and the boundary conditions of the rigid walls read

$$x = 0, 1 - A \le y \le 1 : u = 0, v = 0, \Theta = \Delta T_\parallel/\Delta T_\perp, \tag{10a}$$

$$x = 1, 1 - A \le y \le 1 : u = 0, v = 0, \Theta = 0, \tag{10b}$$

$$x = 0, 0 \le y \le 1 - A : u = 0, v = 0, \partial\Theta/\partial x = 0, \tag{10c}$$

$$x = 1, 0 \le y \le 1 - A : u = 0, v = 0, \partial\Theta/\partial x = 0, \tag{10d}$$

$$y = 0, 0 \le x \le 1 : u = 0, v = 0, \Theta = -1.0, \tag{10e}$$

where $A = h_1/h$, $\Delta T_\perp > 0$.

For the free surface, the capillary number Ca is a measurement of the free surface deformation. In the ZHM model [2], Ca is assumed to be sufficiently small, and thus the surface deformation can be neglected. Under such a case, the free surface can be assumed to be flat, and the boundary condition can be expressed as (to the leading order in Ca)

$$v = 0, \qquad \frac{\partial u}{\partial y} = -\frac{\Delta T_\perp \partial\Theta}{\Delta T_\parallel \partial x}, \qquad \frac{\partial\Theta}{\partial y} = -B_i(\Theta - \Theta_c), \tag{11}$$

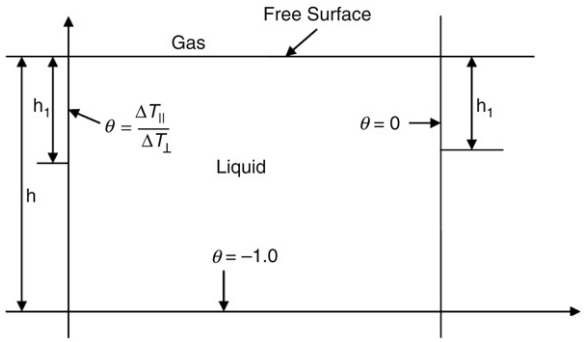

Fig. 1. Geometry of the cavity and boundary condition.

where $B_i = \kappa_g h/\kappa$ is Biot number, κ_g is the gas thermal diffusivity. In our simulations, the surface is adiabatic, and so $B_i = 0$.

The initial velocity is set to be zero at each node with a constant density $\rho_0 = 1.0$. The distribution functions g_i and Θ_i are initialized by setting to the equilibria for all nodes. All simulations are carried out on a 128×128 lattice. The Prandtl number Pr is set to be 0.024 (for Ga melt) and $\Delta T_\perp$ is set to be 1.0.

3.2. Boundary treatment

As we know, the treatment of boundary conditions is crucial in LBM. Many researches have been carried out and several schemes, such as the bounce back scheme [16], the half-way bounce back scheme [17], and the extrapolation scheme [15,18], have been proposed. The detailed analysis about the boundary treatment can be seen in [19].

In the thermocapillary flow in the rectangular cavity, the boundary conditions are complicated, especially for the free surface. Among the schemes for boundary treatment, the non-equilibrium scheme [15] can solve the problem easily, while the others may be quite difficult if not impossible.

Treatments for the boundary conditions on the solid walls using the non-equilibrium scheme can be found in [15]. For the free surface, first we suppose $\mathbf{x}_b$ lies at the free surface and $\mathbf{x}_f$ is the neighboring node in the fluid. Note that the dimensionless temperature Θ_b of the free surface equals Θ_f since $Bi = 0$. Therefore, the velocity u_b of the free surface can be obtained using certain numerical methods. As such, the particle distribution function g_i and Θ_i of the free surface can be obtained according to the non-equilibrium extrapolation scheme,

$$g_i(\mathbf{x}_b, t) = g_i^{\mathrm{eq}}(\mathbf{x}_b, t) + [g_i(\mathbf{x}_f, t) - g_i^{\mathrm{eq}}(\mathbf{x}_f, t)], \tag{12a}$$

$$\Theta_i(\mathbf{x}_b, t) = \Theta_i^{\mathrm{eq}}(\mathbf{x}_b, t) + [\Theta_i(\mathbf{x}_f, t) - \Theta_i^{\mathrm{eq}}(\mathbf{x}_f, t)]. \tag{12b}$$

3.3. Results

Fig. 2 shows the isotherms and the streamlines of the flow for three values of Re, 2.036×10^2, 2.036×10^3, 2.036×10^4 as $\Delta T_\parallel = 0.1, 1.0, 10$ correspondingly. The relaxation parameter $\omega = 1/\tau_u$ is set to be 1.0, 1.5, and 1.95, respectively. To reach the steady state, a number of iterations are performed, where the criterion of steady state is that the difference between the velocities at the center of the cavity for the successive 1000 time steps is less than 5×10^{-6}. As shown, for $Re = 2.036 \times 10^2$, the flow has an influence on the temperature field of the upside of the cavity mostly, and the temperature field is homogeneous in the bottom field. With the increasing of Re, the convection becomes stronger than the diffusion and starts to influence the temperature field in the downside. It is noted that the eddy on the bottom left corner has been calculated but not found by the finite-difference scheme [7]. Table 1 lists the strengths and locations of the vortex of the flow. In Figs. 3 and 4, the temperature and velocity profiles at the free surface are plotted for different Reynolds numbers.

The isotherms of the flow are shown in Fig. 5 with different relative heights of the external temperature on the left wall for $Re = 2.036 \times 10^3$, 2.036×10^4, and 4.072×10^4 with $\Delta T_\parallel = 1.0, 10, 20$. The relaxation parameter $\omega = 1/\tau_u$ is set to be 1.5, 1.95, and 1.97, respectively. It is seen that with the increasing of A, the high temperature field has

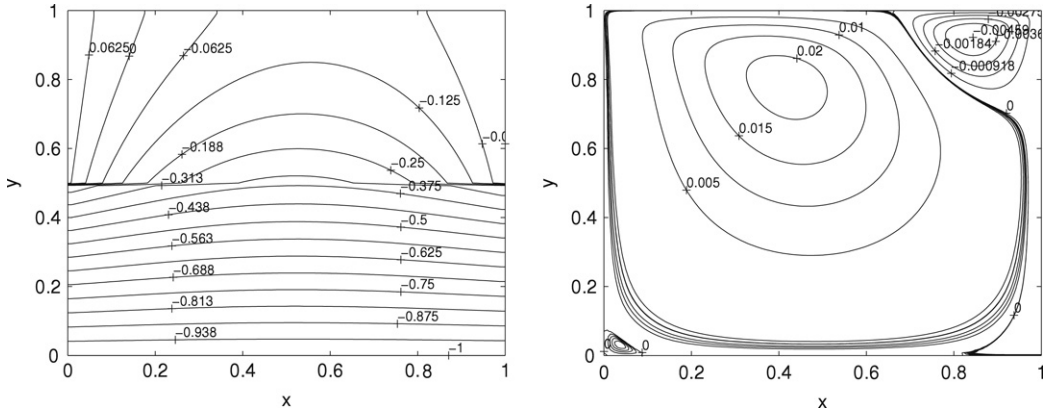

(a) $Re = 2.036 \times 10^2$.

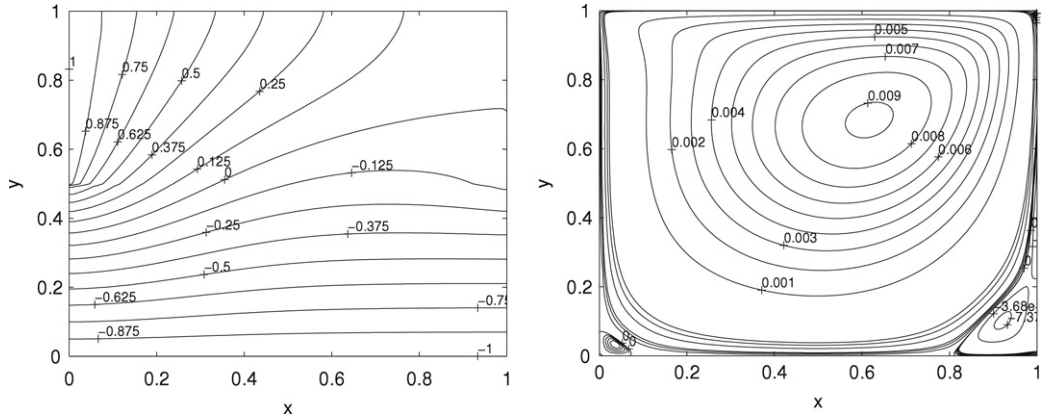

(b) $Re = 2.036 \times 10^3$.

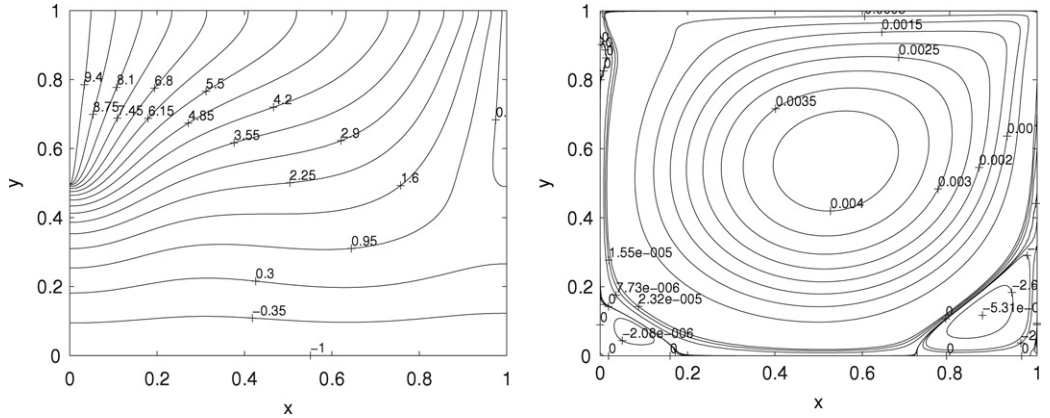

(c) $Re = 2.036 \times 10^4$.

Fig. 2. The isotherms and the stream lines for different *Re* numbers.

been spread downwards and the isotherms become more curved, which implies that the thermocapillary flow has an important influence on the temperature field.

4. Conclusion

In this paper, an LBGK model for the thermocapillary flow has been proposed. The incompressible LBGK model [14] is adopted to describe the velocity field and another LBGK equation is used to model the temperature

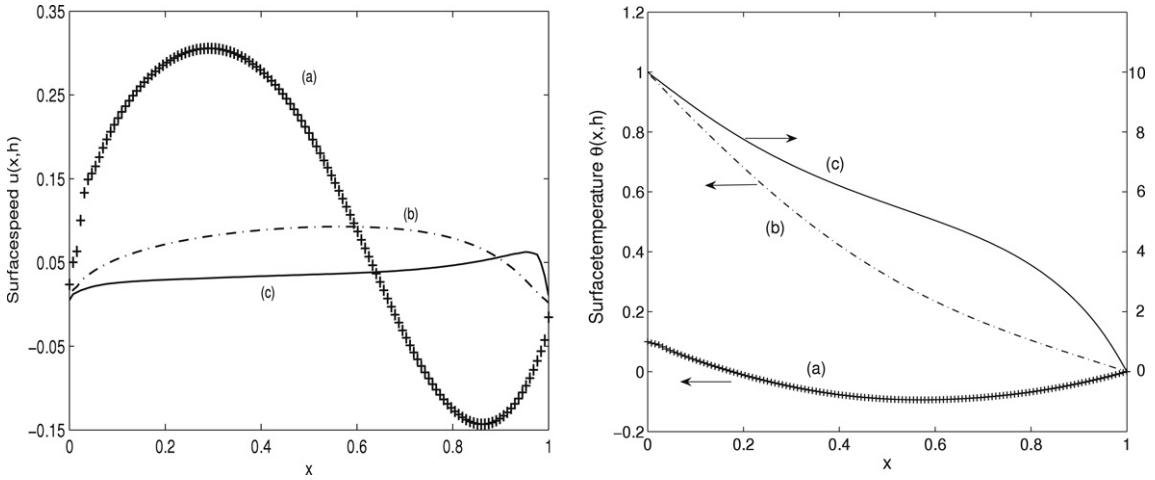

Fig. 3. The speed and temperature along the free surface for different Re number (a) $Re = 2.036 \times 10^2$, (b) $Re = 2.036 \times 10^3$, (c) $Re = 2.036 \times 10^4$.

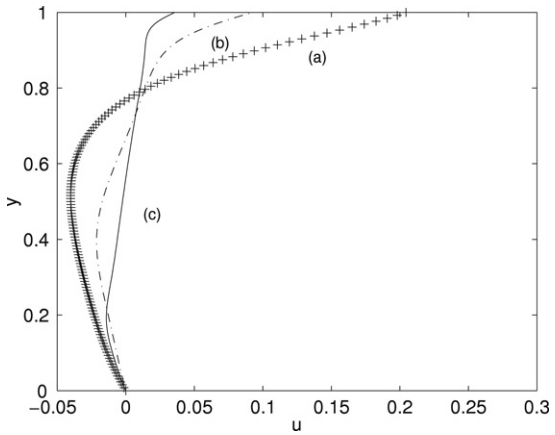

Fig. 4. The speed along Y-direction at $X = 0.5$ for different number (a) $Re = 2.036 \times 10^2$, (b) $Re = 2.036 \times 10^3$, (c) $Re = 2.036 \times 10^4$.

Table 1
Strength and locations of vortex of the flow (φ: vorticity; (x, y): location of the vortex)

Re		φ	x	y
2.036×10^2	Primary	-0.0219	0.4219	0.7091
	Right	0.0046	0.8438	0.9219
	Left	-4.6224×10^{-7}	0.0391	0.0313
2.036×10^3	Primary	-0.0092	0.6172	0.6797
	Right	4.6126×10^{-6}	0.8750	0.1172
	Left	-1.6297×10^{-7}	0.0391	0.0313
2.036×10^4	Primary	-0.0044	0.5391	0.5703
	Right	5.3112×10^{-5}	0.8750	0.1172
	Left	4.1693×10^{-6}	0.0703	0.0703

field. The thermocapillary flow in a rectangular cavity is used to validate the mode. The numerical results agree well with other existing results [7].

It is noted that the free surface is treated as flat under the ZHM assumption. Further studies considering the deflection in the free surface will be carried out in the future.

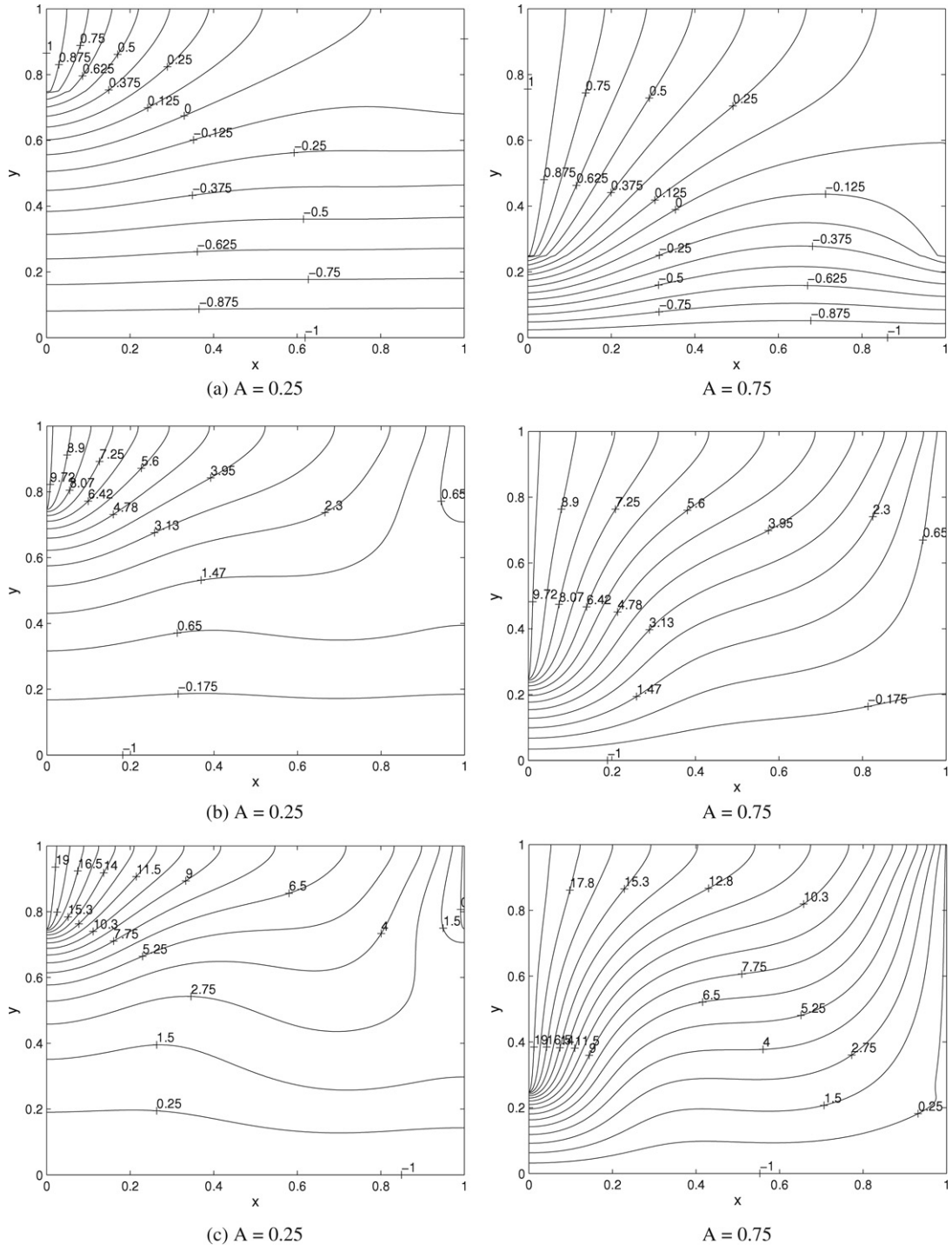

Fig. 5. The isotherms for different *Re* numbers. (a) $Re = 2.036 \times 10^3$, (b) $Re = 2.036 \times 10^4$, (c) $Re = 4.072 \times 10^4$.

Acknowledgments

The authors would like to thank Prof. Zhaoli Guo for helpful discussions. This work is supported by the National Natural Science Foundation of China (Grant No: 70271609).

References

[1] D. Schwabe, Marangoni effects in crystal growth melts, Phys. Chem. Hydrodyn. 2 (1981) 263.
[2] A. Zebib, G.M. Homsy, E. Meiburg, High Marangoni number convection in a square cavity, Phys. Fluids 28 (1985) 3467.
[3] B. Carpenter, G. Homsy, High Marangoni number convection in a square cavity: Part II, Phys. Fluids 2 (1990) 137.
[4] M. Mundrane, J. Xu, A. Zebib, Thermocapillary convection in a rectangular cavity with a deformable interface, Adv. Space Res. 16 (7) (1995) 41.
[5] Chun-Liang Lai, Multiple-scale analysis of Oscillatory thermocapillary convection of high Prandtl number fluids in a rectangular cavity, Int. J. Heat Mass Transfer 47 (2004) 1069.
[6] Z. Zeng, H. Mizuseki, K. Shimamura, et al., Usefullness of experiments with model fluid for thermocapillary convection-effect of Prandtl number on two-dimensional thermocapillary convection, J. Crystal Growth 234 (2002) 272.
[7] L. Zhu, Q. Liu, W. Hu, Thermocapillary convection in low-Prandtl fluid in an open rectangular cavity under microgravity condition, Chinese J. Semicond. 22 (2001) 580.
[8] J. Bhatnagar, E. Gross, M. Krook, A model for collision processes in gases *i*: Small amplitude processes in charged and neutral one-component system, Phys. Rev. 94 (3) (1954) 511.
[9] R. Benzi, S. Succi, M. Vergassola, The lattice Boltzmann equation: Theory and applications, Phys. Rep. 222 (3) (1992) 145.
[10] Y. Qian, S. Succi, A. Orszag, Recent advances in lattice Boltzmann computing, Ann. Rev. Comput. Phys. 3 (1995) 195.
[11] S. Chen, G. Doolen, Lattice Boltzmann method for fluid flows, Ann. Rev. Fluid Mech. 30 (1998) 329.
[12] Z. Guo, B. Shi, C. Zheng, A coupled lattice bgk model for the Bouessinesq equation, Int. J. Numer. Fluids 39 (2002) 325.
[13] B. Shi, Z. Guo, Thermal lattice BGK simulation of turbulent natural convection due to internal heat generation, Internat. J. Modern Phys. B 17 (2003) 173.
[14] Z. Guo, B. Shi, N. Wang, Lattice BGK model for incompressible Navier–Stokes equation, J. Comput. Phys. 165 (2000) 288.
[15] Z. Guo, C. Zheng, B. Shi, An extrapolation method for boundary conditions in lattice Boltzmann method, Phys. Fluids 14 (2002) 2007.
[16] D. Noble, S. Chen, J. Geiorgiadis, R. Buikius, A consistent hydrodynamic boundary condition for the lattice Boltzmann method, Phys. Fluids 7 (1995) 2928.
[17] D. Ziegler, Boundary conditions for lattice Boltzmann simulations, J. Stat. Phys. 71 (1993) 1171.
[18] S. Chen, D. Martinez, R. Mei, On boundary conditions in lattice Boltzmann methods conditions in lattice Boltzmann methods, Phys. Fluids 8 (1996) 2527.
[19] X. Hu, Z. Guo, C. Zheng, Analysis of boundary conditions for lattice Boltzmann model, J. Hydrodynamics, Ser. A 18 (2003) 127.